DOI: 10.1002/adma.200700035

Quantum-Dot-Activated Luminescent Carbon Nanotubes via a Nano Scale Surface Functionalization for *in vivo* Imaging**

By *Donglu Shi*,* *Yan Guo*, *Zhongyun Dong*, *Jie Lian*, *Wei Wang*, *Guokui Liu*, *Lumin Wang*, and *Rodney C. Ewing*

A critical challenge for biomarking, based on luminescent materials, has been the development of nano structures with highly visible or characteristic near infrared emissions for precise imaging, combined with nanoscale cavities for drug storage and delivery. The design of such materials requires complex nanostructures that have both the intense emissions and appropriate storage geometries. We report here a scheme for the use of novel nanostructures designed to satisfy both of these important requirements. Hypodermal and *in vivo* organic imaging from quantum dot conjugated carbon nanotubes has been realized in mice for the first time. The coupling of quantum dots on carbon nanotubes was materialized based on a novel plasma nanotube surface polymerization. The quantum dot activated carbon nanotubes exhibited intense visible light emissions in both fluorescent spectroscopy and *in vivo* imaging. These experimental results can be extended to the development of new techniques for early cancer diagnosis.

There is an increasing need for the early detection of cancer, prior to the detection of anatomic anomalies. Thus, a major challenge in cancer diagnosis is to locally biomark cancer cells for maximum therapeutic benefit.[1,2] In cancer therapy, the targeting and localized delivery of drugs are also key challenges. One promising strategy for overcoming these challenges is to make use of highly luminescent nanoparticles for qualitative or quantitative *in vitro* detection of tumor cells.[3–8] Recently, *in vivo* imaging using single wall carbon nanotubes has also been reported.[9,10] In the cancer diagnosis and treatment by nanotechnology, it has been critical to develop novel nanostructures that combine multiple functionalities including biocompatibility, fluorescent signaling, drug storage and delivery, and coupling to biological molecules such as DNA/RNA, antibodies, and viruses. In the design of such a complex nanostructure, nanotubes of a variety of materials may serve as ideal substrates, on which multifunctional structures needed for biomedical diagnosis and treatment can be developed.

Based on above considerations, we report a novel nanotube surface design ideally suited for this purpose. In contrast to previous studies, this novel nano system was materialized via several unique synthesis routes including plasma surface functionalization. The hollow center of the nanotube can be filled with a cancer treatment drugs. The outer surface of the nanotube is coated with luminescent materials for enhanced optical properties. Although carbon nanotubes are known to have near-infrared emissions, the luminescence intensities are generally too weak for whole-body *in vivo* imaging. Therefore, intense emissions and tunable wavelengths can only be provided by luminescent materials such as quantum dots (QDs). Compared with other traditional, rare-earth-doped semiconductors[11] and organic fluorophores,[12] QDs have superior properties, including higher quantum yield with a broader emission spectrum than that of rare earth phosphors. In addition, the spectra are much sharper than the emission spectra of organic fluorophores.[3–9] QDs are semiconducting nanocrystals that possess size-tunable electronic and optical properties resulting from quantum confinement effects.[13,14] They offer high resistance to photo-bleaching, thus making them attractive materials for optoelectronics[15,16] and *in vivo* biosensing applications.[17] After the chemical treatment, the QDs go into the lighter aqueous phase. This ensures the synthesis of water-soluble QDs with functional groups, such as QD-NH_2 and QD-COOH.

Due to the chemical inertness of carbon nanotubes, their surface modification must be completed in order to attach the QDs. For instance, the acid oxidation of carbon nanotubes, resulting in the carboxyl groups at the tips and other high defect

[*] Prof. D. Shi, Y. Guo, W. Wang
Department of Chemical and Materials Engineering
University of Cincinnati
Cincinnati, OH 45221 (USA)
E-mail: shid@email.uc.edu
Prof. D. Shi
Research Institute of Micro/Nano Science & Technology
Shanghai Jiao Tong University
Shanghai, 200030 (P. R. China)
Prof. Z. Dong
Department of Internal Medicine, College of Medicine
University of Cincinnati
Cincinnati, OH 45267 (USA)
Dr. J. Lian, Prof. L. Wang, Prof. R. C. Ewing
Departments of Geological Sciences, Nuclear Engineering & Radiological Sciences and Materials Science & Engineering
University of Michigan
Ann Arbor, MI 48109 (USA)
Dr. G. Liu
Chemistry Division
Argonne National Laboratory
Argonne, IL 60439 (USA)

[**] The work performed at University of Cincinnati was supported by a grant from the Institute for Nanoscale Science and Technology, University of Cincinnati. The TEM analyses were conducted at the Electron Microbeam Analysis Laboratory at the University of Michigan and supported by an NSF NIRT grant (EAR-0403732).

ADVANCED MATERIALS

density sites was one of the effective approaches.[18] The direct covalent functionalization was based on the reaction between carboxyl and amine. In this study a unique plasma coating method was developed in order to generate the carboxyl functional groups on multi-wall carbon nanotubes (MWCNTs-COOH) for covalent coupling to CdSe/ZnS quantum dots. These quantum dots were functionalized with amine (QD-NH_2).[19–23] The coupling procedure to obtain the MWCNTs-QDs heterostructures is illustrated in Figure 1.

The MWCNTs were chosen for their larger inner wall diameters (70–150 nm). This dimension of MWCNTs is particularly suitable for several anti-cancer drugs with comparable molecular sizes.[24] The drug storage study is, however, not included in this experiment, but being carried out in a subsequent investigation currently underway. The toxicity and biocompatibility of carbon nanotubes have been previously studied.[25,26] After successfully demonstrating the concept of nano-biomarker using MWCNTs, other more biodegradable substrates maybe selected for the same application. A novel surface functionalization method was employed to uniformly deposit ultra-thin films of functional groups on MWCNTs in order to attach luminescent materials on their surfaces. The purpose of *in vivo* imaging experiments in this research was to demonstrate the feasibility of the quantum dots activated MWCNTs in biomedical diagnosis. The present research is primarily centered on the design of the surface nanostructures, development of luminescent carbon nanotubes, and their corresponding physical properties.

Plasma polymerization is a novel and effective method for surface functionalization of nanotubes and nanoparticles.[19–23] The main principle of the plasma polymerization is that the ionized and excited monomer molecules created by the electrical field bombard and react on the surface of the substrate. These activated molecules may etch, sputter, or deposit on the substrate surface. Due to these characteristics, the plasma technique can be used for polymer surface functionalization on various nanotubes and nanoparticles. The experimental procedures and conditions for plasma surface functionalization and characterization have been previously published.[19–23] The plasma reactor for surface functionalization consists mainly of a radio-frequency source, the glass vacuum chamber, and pressure gauge. The monomers were introduced from the gas inlet during the plasma polymerization. In this study, acrylic acid (AA) monomer was used for the surface functionalization of the nanotubes.

Figure 2 shows the high resolution transmission electron microscopic (HRTEM) images of surface functionalized MWCNTs. An ultrathin AA film of 2 nm can be clearly seen on the outer surface of the nanotube after plasma polymerization (Fig. 2a). The carbon lattice imaging can also be seen in this figure, which is in contrast to the amorphous AA film. In Figure 2b, similar AA film can be seen, but near the open end of the nanotube. The AA film appears quite uniform covering the outer surface of the nanotube. In Figure 2b, it can be seen that the nanotube has an open end, thus particularly suitable for storage of drugs. The plasma deposited surface films on nanotubes and nanoparticles have been characterized by secondary ion mass spectroscopy and infrared spectroscopy. The surface analysis results are not shown in this study but can be found in ref. [19–23].

To study the luminescence behavior of MWCNTs-QDs, fluorescent microscopy was carried out. A drop of MWCNTs-QDs suspension was smeared on a glass slide for fluorescent microscopy observed using an Olympus 1X51 with the excitation of 350 nm. The MWCNTs were well below the diffraction-limited resolution of the optical system. Figure 3 shows the fluorescent and transmitted-bright field image of the

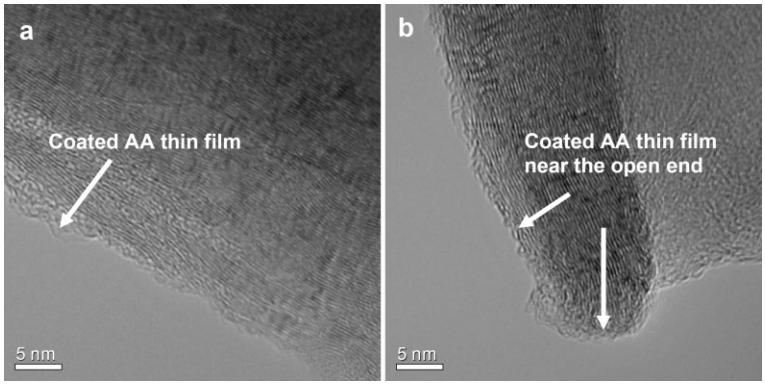

Figure 2. TEM images showing a) the plasma deposited acrylic acid (AA) polymer thin film on the carbon nanotube, the lattice image of carbon nanotube can be clearly seen with an extremely thin layer of polymer film (~ 2 nm); b) the thin film of AA was plasma deposited near the open end of the carbon nanotube.

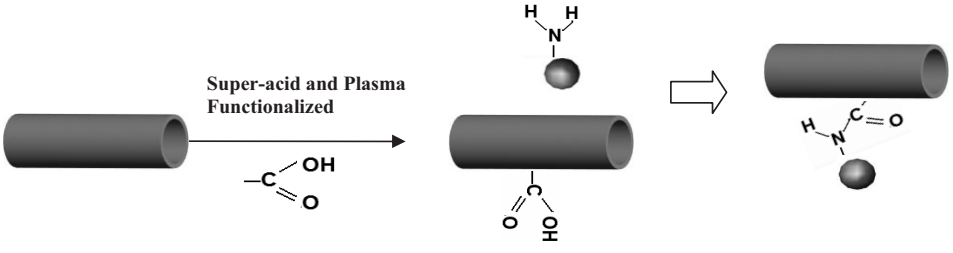

Figure 1. Schematic diagram showing the procedure for coupling the carboxyl functionalized MWCNTs with amine functionalized CdSe/ZnS quantum dots.

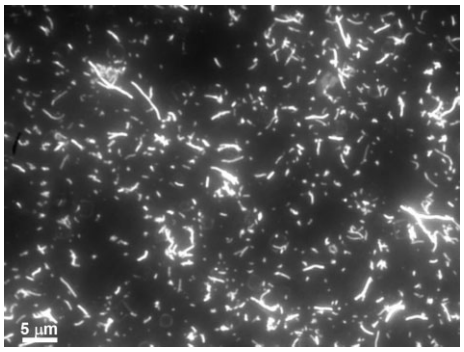

Figure 3. Fluorescent microscopy image (Olympus 1X51 under the 350 nm excitation) showing that the MWCNTs are individually labeled with fluorescent QDs and exhibiting strong emissions against the dark background.

MWCNTs-QDs sample. The MWCNTs were individually spread across the slide and are labeled with fluorescent QDs over entire surface area. Each nanotube exhibits strong emissions against the dark background, the spectra of which were further analyzed by a laser fluorescent spectrometer.

The laser excitation experiment was completed at room temperature and a Nd:YAG pulse laser at 355 nm was used to "pump" the samples. Figure 4 shows the luminescence spectrum observed at room temperature from the MWCNTs conjugated with CdSe/ZnS. The peak is broad with a maximum around 610 nm. A small red shift is evident in Figure 4 as compared with the emission of pure quantum dots, where the peak intensity is at 600 nm (data not shown here). In comparison with rare earth phosphors, the peak of the QDs luminescence spectrum is similar to the Eu^{3+} spectrum, which has emission peaks from 590 to 620 nm, with the strongest peak of the $^5D_0 \rightarrow {}^7F_2$ transition near 610 nm.[27,28] The present results show that the quantum efficiency of the MWCNTs-QDs is much higher than that of the Eu^{3+}:Y_2O_3-HA.[28] This may be understood based on the parity forbidden f–f transitions in rare earth ions. It was more important in the present study that the QDs luminescence would not be quenched when the

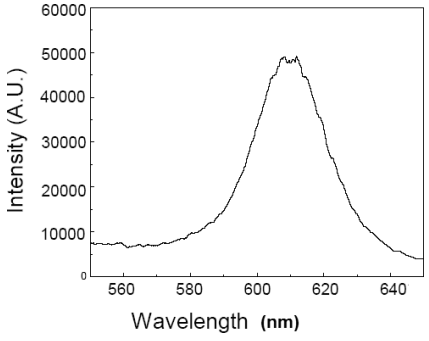

Figure 4. Fluorescence emission spectra of the MWCNTs-QDs at room temperature. As shown, a maximum peak around 610 nm was observed. It is evident there is a small red shift of MWCNTs-QDs compared to the emission of the pure QDs, where the peak is at 600 nm (data not shown here).

MWCNTs-QDs particles were diluted in phosphate-buffered saline (PBS) solution and injected *in vivo*. This is a significant advantage for biomedical applications.

Figure 5a shows a bright-field TEM image of the MWCNTs-QDs. The TEM samples were prepared by dispersing the MWCNTs-QDs suspension directly on holy-carbon films supported with Cu grids. As can be seen in Figure 5, the quantum dots show a dark contrast and a particle size of 5–10 nm, randomly distributed on the surface of the nanotubes (Fig. 5a). High-resolution TEM images (Fig. 5b and c) clearly show the crystalline CdSe/ZnS quantum dots depos-

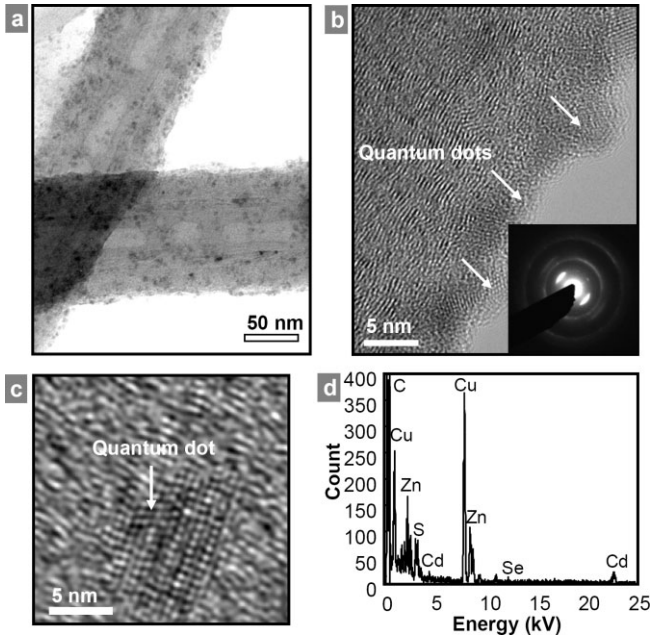

Figure 5. a) TEM image of carbon nanotubes with surface coupled quantum dots; b) and c) are HRTEM images of the crystalline CdSe/ZnS quantum dots deposited on the side walls of carbon nanotubes. The inset of Figure 5b is the selected area electron diffraction pattern acquired from the surface functionalized carbon nanotubes; (d) the energy dispersive X-ray spectrum acquired from the functionalized carbon nanotubes showing the signals from CdSe/ZnS quantum dots.

ited on the surfaces of the carbon nanotubes. The interlayer of (002) of the carbon nanotubes are clearly resolved in both HRTEM images. The inset of Figure 5b is the selected area electron diffraction pattern acquired from the surface-functionalized carbon nanotubes. The diffuse diffraction maxima correspond to diffraction from the (002) graphite layer of the carbon nanotubes, and the ring patterns can be indexed to the structures of the CdSe/ZnS quantum dots. The energy dispersive X-ray spectrum acquired from the functionalized carbon nanotubes (Fig. 5d) shows the signals from the CdSe/ZnS quantum dots, consistent with the TEM observations.

As an initial step in exploring potential biological applications of this novel method, the visibility of MWCNTs-QDs was tested in mice. This *in vivo* imaging test by direct injection

ADVANCED MATERIALS

was a necessary step before the experiment via intravenous route as obtaining visible images of MWCNTs-QDs in mice has been a challenging task in the past. The 0.01 ml of MWCNTs-QDs (0.5 μg ml^{-1} in PBS) were injected into anesthetized nude mice and the luminescence was detected by using the Kodak Image Station In-Vivo Imaging System. To excite the emission of MWCNTs-QDs, an epi-UV illuminator was used. This source provided adequate excitation and minimal auto-fluorescence. The mice were placed into a whole-mouse imaging system. The 435 nm excitation light, from a high-intensity lamp with the 10× zoom lens, was directed through the selected excitation filter to the mice. Fluorescence emitted from the quantum dots inside the animal was detected with the CCD camera and digitized to a computer.

The mice hypodermic injections including the mid-dorsal and abdomen regions were performed (Fig. 6a and b). The images were collected after exposures of 2 minutes. The suspensions of MWCNTs-QDs were diluted by PBS at different concentrations (0.5 μg ml^{-1}, 0.25 μg ml^{-1}, 0.125 μg ml^{-1}, 0.083 μg ml^{-1} and 0.0625 μg ml^{-1}). As an initial *in vivo* test of the MWCNTs-QDs, 0.01 ml of the suspension was injected into various ventrolateral locations from head to the tail (Fig. 6b). As can be seen in Figure 6b, the fluorescence intensities correlate directly to the concentrations of the MWCNTs-QDs administered to the mice (Fig. 6b). For concentrations above 0.125 μg ml^{-1}, the images all exhibit pronounced fluorescence intensities (location A, B, and C). Even for an extremely low concentration of 0.0625 μg ml^{-1} (location E), the luminescent image could still be visualized indicating that the MWCNTs-QDs can be easily traced in live animals.

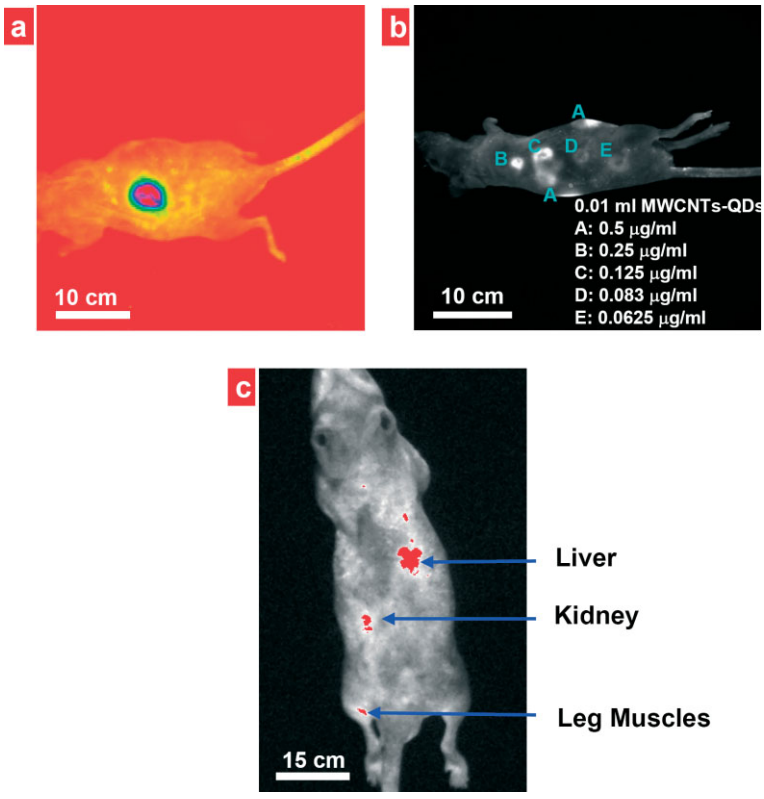

Figure 6. *In vivo* images of MWCNTs-QDs (0.5 μg ml^{-1} in PBS) in mice injected at different body regions: a) MWCNTs attached with CdSe/ZnS quantum dots (emission of 600 nm) at middorsal location; b) MWCNTs attached with CdSe/ZnS quantum dots at ventrolateral locations, the suspensions were diluted by PBS at various concentrations as indicated (A through E); c) MWCNTs attached with InGaP/ZnS quantum dots (emission of 680 nm, 0.25 μg ml^{-1} in PBS) in liver, kidney, and leg muscles. All images were taken successively in 2 min under epi-UV illuminator with excitation of 435 nm.

For a comparative study, we substituted quantum dots of CdSe/ZnS on the nanotubes with InGaP/ZnS which has a considerably longer emission wavelength of 680 nm. All surface functionalization and conjugation procedures applied were the same as described before. Figure 6c is the *in vivo* image resulting from the InGaP/ZnS quantum dots activated carbon nanotubes. The suspension with the concentration of 0.25 μg ml^{-1} in PBS was directly injected into liver, kidney, and leg muscles. Figure 6c is the view from the back of the mouse, and the image is much brighter that those obtained from CdSe/ZnS quantum dots with a shorter wavelength. In contrast to images from under-skin injections of MWCNTs-QDs as shown in Figure 6a and b, Fig. 6c is the image from the deep tissue injections in targeted organs. These results clearly demonstrate the intense fluorescent signals of MWCNTs-QDs in the entire body.

From the data shown in Figure 6, a conclusion can be drawn that the longer emission wavelength in the near-infrared region is preferable for the diagnosis experiment. Emissions in the visible range below 600 nm can easily overlap with those from the animal bodies as a background noise, resulting in a reduced contrast. However, much longer emissions between 700 nm and 800 nm would be ideal for the diagnostic imaging purposes. Therefore, using the nano surface design described in this study, when combined with multiple wave-length co-registrations, these fluorescent MWCNTs-QDs should be able to probe tumor burdens with anatomical localization and, potentially, selectively deliver drugs into the tumor lesions. *In vivo* imaging with MWCNTs-QDs of much longer emissions via intravenous route and drug storage experiments are currently underway.

Based on a novel nanostructure design, quantum dots were conjugated onto the outside surfaces of the MWCNTs for the purpose of cancer diagnosis and potential treatment protocols. A unique plasma polymerization method was employed to deposit ultra-thin films of functional groups on the MWCNTs surfaces, with which the quantum dots were effectively conjugated. The MWCNTs-QDs exhibited strong luminescent emissions in the visible light range that were observed *in vivo* for the first time. It was found that quantum dots with longer wavelengths exhibited much brighter imaging for deep tissue

diagnosis. These clear *in vivo* images obtained from the MWCNTs-QDs indicate that this novel nanoscale design can be used as an effective biomarker for biomedical applications. Hence, these materials may find important applications in the cancer diagnosis and treatment.

Experimental

EviTags 600 CdSe/ZnS quantum dots (emission wavelength of 600 nm) with hydrodynamic diameters of 40 nm were purchased from Evident Technologies. They were functionalized with amine and kept in water with the concentration of 10–12 (nmols ml^{-1}). Commercial grade multi-wall carbon nanotubes (MWCNTs) were provided by Applied Science Inc. as substrates in this experiment. These MWCNTs were 70–150 nm in diameter and several micrometers in length. In this experiment, the surfaces of MWCNTs were treated first by superacid (HNO_3 + H_2SO_4). A thin film (< 5 nm) was then deposited by plasma polymerization onto their surfaces in order to provide the carboxyl functional groups. After surface functionalization, the MWCNTs were dispersed into phosphate buffered saline solution (PBS) with a concentration of 35 μmol ml^{-1}.

To obtain the MWCNTs-QDs heterostructures, the coupling procedure was employed by using stabilizers of 1-(3-dimethylaminopropyl)-3-ethylcarbodiimide hydrochloride in the presence of *N*-hydroxysuccinimide. The reaction was completed in PBS at pH 7.4. The MWCNTs-QDs suspension was incubated at 42 °C for 8 hours. The MWCNTs-QDs suspension was cooled to room temperature, centrifuged for 30 min, and rinsed three times with PBS using centrifugation and decantation. The coupled MWCNTs-QDs suspension was filtered through a 3.0 μm teflon membrane and re-suspended in PBS. The ratio of QDs to MWCNTs was kept in the range between 1:1 and 1:4 (volume ratio).

The mice used for *in vivo* imaging were maintained in a facility approved by the American Association for Accreditation of Laboratory Animal Care and in accordance with current regulations and standards of the U. S. Department of Agriculture, U. S. Department of Health and Human Services, and National Institute of Health. This study was approved by Institutional Anima Use and Care Committee (IACUC) at the University of Cincinnati, OH.

Received: January 5, 2007
Revised: June 26, 2007
Published online: October 31, 2007

[1] D. R. Walt, *Science* **2005**, *308*, 217.
[2] M. Ferrari, *Nat. Rev. Cancer* **2005**, *5*, 161.
[3] X. Gao, Y. Cui, R. M. Levenson, L. W. K. Chung, S. Nie, *Nat. Biotechnol.* **2004**, *22*, 969.
[4] B. Dubertret, P. Skourides, D. J. Norris, V. Noireaux, A. H. Brivanlou, A. Libchaber, *Science* **2002**, *298*, 1759.
[5] X. Wu, H. Liu, J. Liu, K. N. Haley, J. A. Treadway, J. P. Larson, N. Ge, F. Peale, M. P. Bruchez, *Nat. Biotechnol.* **2003**, *21*, 41.
[6] J. K. Jaiswal, H. Mattoussi, J. M. Mauro, S. M. Simon, *Nat. Biotechnol.* **2003**, *21*, 47.
[7] D. R. Larson, W. R. Zipfel, R. M. Williams, S. W. Clark, M. P. Bruchez, F. W. Wise, W. W. Webb, *Science* **2003**, *300*, 1434.
[8] A. M. Derfus, W. C. W. Chan, S. N. Bhatia, *Nano Lett.* **2004**, *4*, 11.
[9] P. Cherukuri, C. J. Gannon, T. K. Leeuw, H. K. Schmidt, R. E. Smalley, S. A. Curley, R. B. Weisman, *Proc. Natl. Acad. Sci. USA* **2006**, *103*, 18882.
[10] Z. Liu, W. Cai, L. He, N. Nakayama, K. Chen, X. Sun, X. Chen, H. Dai, *Nat. Nanotechnol.* **2007**, *2*, 47.
[11] X. Y. Chen, L. Yang, R. E. Cook, S. Skanthakumar, D. Shi, G. K. Liu, *Nanotechnology* **2003**, *14*, 670.
[12] V. Väisänen, H. Härmä, H. Lilja, A. Bjartell, *Luminescence* **2000**, *15*, 389.
[13] L. Brus, *Appl. Phys. A* **1991**, *53*, 465.
[14] A. P. Alivisatos, *J. Phys. Chem.* **1996**, *100*, 13226.
[15] S. Banerjee, S. S. Wong, *Nano Lett.* **2002**, *2*, 195.
[16] J. M. Haremza, M. A. Hahn, T. D. Krauss, *Nano Lett.* **2002**, *2*, 1253.
[17] W. C. W. Chan, S. Nie, *Science* **1998**, *281*, 2016.
[18] A. G. Rinzler, J. Liu, H. Dai, P. Nikolaev, C. B. Huffman, F. J. Rodríguez-Macías, P. J. Boul, A. H. Lu, D. Heymann, D. T. Colbert, R. S. Lee, J. E. Fischer, A. M. Rao, P. C. Eklund, R. E. Smalley, *Appl. Phys. A* **1998**, *67*, 29.
[19] D. Shi, P. He, J. Lian, L. M. Wang, D. Mast, M. Schulz, *Appl. Phys. Lett.* **2002**, *81*, 5216.
[20] D. Shi, S. X. Wang, W. J. Van Ooij, L. M. Wang, J. G. Zhao, Z. Yu, *Appl. Phys. Lett.* **2001**, *78*, 1243.
[21] D. Shi, P. He, J. Lian, L. M. Wang, D. Mast, M. Schulz, *Appl. Phys. Lett.* **2003**, *83*, 5301.
[22] D. Shi, P. He, J. Lian, L. M. Wang, W. J. Van Ooij, *J. Mater. Res.* **2002**, *17*, 2555.
[23] P. He, D. Shi, J. Lian, L. M. Wang, R. C. Ewing, W. J. Van Ooij, Z. Li, Z. F. Ren, *Appl. Phys. Lett.* **2005**, *86*, 043107.
[24] C. F. Shaw III, *Chem. Rev.* **1999**, *99*, 2589.
[25] G. Jia, H. Wang, L. Yan, X. Wang, R. Pei, T. Yan, Y. Zhao, X. Guo, *Environ. Sci. Technol.* **2005**, *39*, 1378.
[26] C. W. Lam, J. T. James, R. McCluskey, R. L. Hunter, *Toxicol Sci.* **2004**, *77*, 126.
[27] D. Shi, J. Lian, W. Wang, G. K. Liu, P. He, Z. Dong, L. M. Wang, R. C. Ewing, *Adv. Mater.* **2006**, *18*, 189.
[28] W. Wang, D. Shi, J. Lian, G. K. Liu, P. He, Z. Dong, L. M. Wang, R. C. Ewing, *Appl. Phys. Lett.* **2006**, *89*, 183106.

